Geological Quarterly, 2025, 69, 37
DOI: https://doi.org/10.7306/gq.1810

Salt mineral crystallization features in the Dawenkou Basin, China: insights from brine fluid inclusions in halite

Anatoliy R. GALAMAY[1], Fanwei MENG[2, 3], Krzysztof BUKOWSKI[4, *], Wentao CHEN[5] and Le LI[6]

[1] Institute of Geology and Geochemistry of Combustible Minerals, NAS of Ukraine, 3a Naukova Street, Lviv, 79060, Ukraine; ORCID: 0000-0003-4864-6401

[2] China University of Mining and Technology, School of Resources and Earth Sciences, no. 1 Daxue Road, Xuzhou, Jiangsu, 221116, China; ORCID: 0000-0003-1994-0812

[3] Chinese Academy of Sciences, Qinghai Institute of Salt Lakes, 18 Xinning Road, Xining, Qinghai, 810008, China

[4] AGH University, Faculty of Geology, Geophysics and Environment Protection, al. Mickiewicza 30, 30-059 Kraków, Poland; ORCID: 0000-0001-7289-5956

[5] Shandong Institute of Geological Sciences, Lishan Road 52, Jinan, Shandong Province, 250013, China

[6] Shandong Luyin Energy Storage Engineering Technology Co., Ltd, Taian 271000, China

Galamay, A.R., Meng, F., Bukowski, K., Chen W., LI. L., 2025. Salt mineral crystallization features in the Dawenkou Basin, China: insights from brine fluid inclusions in halite. Geological Quarterly, **69**, 37; https://doi.org/10.7306/gq.1810

The Dawenkou Basin in China is a significant Cenozoic evaporite basin containing a diverse range of salt minerals, including halite, anhydrite, glauberite, polyhalite, and various Na-Mg and K-Mg salts. This study investigates the origins of brines that contributed to salt formation in the basin, as well as the sedimentary and post-sedimentary mineralization processes, through fluid inclusion analysis in halite and sulphur-oxygen isotopic studies in anhydrite. Analysis of fluid inclusions in halite from well XZK 101 revealed both primary and secondary inclusions, with evidence of tectonic activity, recrystallization, and fluid migration. Brine compositions vary widely, with K^+, Mg^+, and SO_4^{2-} concentrations indicating multiple stages of mineral formation and alteration. The presence of hydrocarbons and algal remnants in inclusions suggests interactions with organic material during or after salt deposition. Isotopic data (^{34}S and ^{18}O) from anhydrite show values suggesting the primary sulphate source was leached from Cambrian and Ordovician evaporites in the surrounding Yi-Meng Mountains, rather than solely from marine sources. The chemical and isotopic composition of the brines does not exclude the influence of marine transgressions during the Eocene, although the dominant input of sulphate appears to come from continental sources. The complex interplay between marine influx, tectonic processes, and continental sulphate leaching shaped the unique salt mineral assemblage observed in the basin today.

Key words: halite, anhydrite, fluid inclusions, stable isotopes, Dawenkou Basin.

INTRODUCTION

One of the principal challenges in the geochemical study of evaporites is distinguishing between marine evaporites (derived from seawater) and continental evaporites, which originate from land-derived waters in which the relative proportions of major ions may or may not differ from those in seawater. A notable example is the Great Salt Lake in Utah, USA, where continental brines closely resemble seawater brines (Drever, 1997). Despite several differences, distinguishing ancient marine evaporites from those of continental origin is often challenging. Sedimentological, micropalaeontological, mineralogical, and geochemical criteria (Hardie, 1984; Sonnenfeld and Hardie, 1985; Lowenstein and Hardie, 1985; Bąbel and Schreiber, 2014) do not always allow for a clear distinction between the two types.

Salt minerals in evaporite basins can be broadly categorized as either marine or continental, depending on the brine's source. However, many minerals are found in both environments, commonly making such classification ambiguous or complex. The mineral assemblage of marine evaporites reflects systematic variations in seawater chemistry throughout the Phanerozoic, ranging from Na-K-Mg-Cl-SO_4 (SO_4-rich) to Na-K-Mg-Ca-Cl (Ca-rich) types (Zimmermann, 2000; Lowenstein et al., 2001, 2003; Bąbel and Schreiber, 2014).

In SO_4-rich seawater, evaporation results in the sequential precipitation of minerals as the brine becomes increasingly concentrated: calcite and gypsum are followed by halite; halite with epsomite and sylvite; halite with hexahydrite and sylvite; halite

* Corresponding author, e-mail: buk@agh.edu.pl

Received: August 21, 2025; accepted: September 20, 2025; first published online: November 13, 2025

with hexahydrite and carnallite; and eventually halite with carnallite and bischofite (Lowenstein et al., 2003). At elevated temperatures (e.g., 55°C), additional minerals, such as langbeinite, kieserite, and kainite, may also crystallize (Horita et al., 2002).

During diagenesis, interactions with sedimentary brines alter the primary mineral assemblages. These changes lead to the formation of new, more stable minerals that are in equilibrium with the evolved intercrystalline brines. Processes such as the dehydration of crystalline hydrates and the transformation of metastable minerals result in sylvite, langbeinite, kainite, polyhalite and kieserite becoming dominant rock-forming minerals in sulphate-type potash deposits. In Ca-rich seawater, the crystallization sequence differs and typically includes halite, sylvite, carnallite, tachyhydrite and bischofite (Valyashko, 1962).

Continental evaporite assemblages are typically more mineralogically diverse than their marine counterparts and commonly include heterogeneous layers with unique salt compositions (Kovalevich, 1990; Horita et al., 2002). Nevertheless, distinctions between marine and continental halogenesis can be subtle. Minerals such as langbeinite, kieserite and carnallite – commonly associated with marine evaporites – can also form in continental settings if sufficient K and Mg are leached from the watershed of an interior basin (Strakhov, 1962; Petrichenko, 1988). The genesis of mineral assemblages containing salts from advanced stages of brine concentration remains a subject of active debate in salt geology. Beyond reconstructing palaeoclimatic and palaeotectonic conditions, this problem requires information on the sources of the salt and the nature and mechanisms of secondary processes that affect salt-bearing strata. A key approach involves comparing the chemical composition of sedimentary brines with that of seawater from the corresponding geological period, often through diagrammatic methods (Stankevich et al., 1991; Horita et al., 2002). Analyses of primary fluid inclusions in halite (formed prior to potash deposition in marine settings) and in bloedite (characteristic of continental evaporites) are especially valuable, as ionic ratios in sedimentary brines remain stable throughout the halite precipitation stage (Horita et al., 2002; Kovalevych et al., 2009).

Particular emphasis is placed on the study of halite-hosted fluid inclusions, which serve as critical indicators of evaporite origin. Primary inclusions form during halite crystallization at the brine-air interface, on the basin floor, or in mixing zones of brines with different densities. Secondary inclusions result from post-sedimentary processes or the refilling of earlier inclusions (McCaffrey et al., 1987). These inclusions preserve information on the physicochemical conditions that prevailed during sedimentation or subsequent recrystallization. As such, they provide some of the most reliable data for determining the origin of salts in a basin and the characteristics of halogenesis. Numerous studies have demonstrated the high informational value of these inclusions (Benison and Goldstein, 1999; Zimmermann, 2000; Lowenstein et al., 2001, 2003; Petrychenko et al., 2006; Kovalevych et al., 2012; Vovnyuk et al., 2017; Galamay et al., 2020, 2021a).

The Dawenkou Basin, the largest salt-bearing basin in western Shandong Province, is a Cenozoic terrestrial fault basin (Wang et al., 2021). It contains beds of rock salt interbedded with layers of anhydrite and silty dolomite, along with sequences containing glauberite, thenardite, aphthitalite, polyhalite, Na-Mg salt minerals (leonite, vanthoffite, bloedite), and K-Mg salt minerals (kieserite, langbeinite). This study aims to identify the sources of brines that fed the Dawenkou Basin and to examine the characteristics of sedimentary and post-sedimentary mineral formation, utilizing thermobarogeochemical analysis of fluid inclusions in halite and isotopic data from anhydrite.

GEOLOGICAL SETTING

The Dawenkou Basin is an evaporite basin located in Shandong Province. Although it covers only 320 km^2 and is small compared to other sedimentary basins in eastern China, it contains 15 billion tons of gypsum over an area of 135 km^2, 1.5 billion tons of halite in an area of 36 km^2, 9 million tons of potassium-magnesium salts in an area of 5 km^2, and 0.25 billion tons of native sulphur in an area of 40 km^2 (Wang et al., 2003). The Dawenkou Formation exceeds 3000 m in thickness. Several distinct sedimentary facies are present, including clastic, carbonate, sulphate, halite, and potassium-magnesium (Song, 2010). Rock salt members are up to 345 m thick.

The formation is divided into three parts:

- lower part, represented by conglomerates (ranging from boulder-bearing to sandy) in a greyish-green and purple-red muddy matrix with a thickness of ~500 m;
- middle part (which is evaporite), with a thickness of 1500 m;
- upper part, represented by marls interbedded with sandstones and occasionally with anhydrite, with a thickness of 930 m.

The middle part of the formation is further divided into three layers: lower anhydrite, middle halite and upper anhydrite (Song, 2010; Zhu, 2015). The salt mass consists of rock salt deposits intercalated with layers of anhydrite and silty dolomite, as well as layers containing glauberite, thenardite, aphthitalite, polyhalite, Na-Mg salt minerals (leweite, vanthofite, bloedite), and K-Mg salt minerals (kieserite, langbeinite). The sources of salt in the Dawenkou Basin remain a matter of controversy.

The basin is adjacent to the larger Bohai Gulf Basin, which may have accumulated sediment during marine transgression into North China during the Cretaceous and Eocene. Therefore, a marine origin for the Dawenkou evaporites is possible (Fig. 1). Recent studies of the chemical composition of brine inclusions in halite from the Jintan Basin, located south of the Dawenkou Basin, have demonstrated the marine origin of the lower salt layer (Meng et al., 2020). Meanwhile, marine fossils within the salt component of the Dawenkou Formation are rare, including radiolarians (found in the Wenkou Depression), bryozoans, and foraminifera (found in wells ZK-5 and ZK-14 of the Wenkou Depression; Li, 1986; Ren et al., 2000; Wu and Ren, 2004). In the sandstones of the middle part of the Dawenkou Formation in well ZK-9, minerals of the glauconite group were discovered (Zhu, 2015). The location of these wells in the Dawenkou Basin is shown in Figure 2. However, the issue of marine transgressions during the Cretaceous-Eocene time interval remains hotly debated, primarily due to the fragmentary and ambiguous interpretation of the micropalaeontological data and the lack of data on the chemical composition of the sedimentary brines in the basins.

MATERIALS AND METHODS

The XZK 101 borehole, from which halite and anhydrite samples for this research were obtained, was drilled in 2018 by the Geological Survey of Southern Shandong (China) near the city of Manzhuang in the Wenkou Depression (see Fig. 2). Halite sample DWK-07 was taken from a depth of 935.3 m (from the bottom of the lowest rock salt layer). Halite sample DWK-09

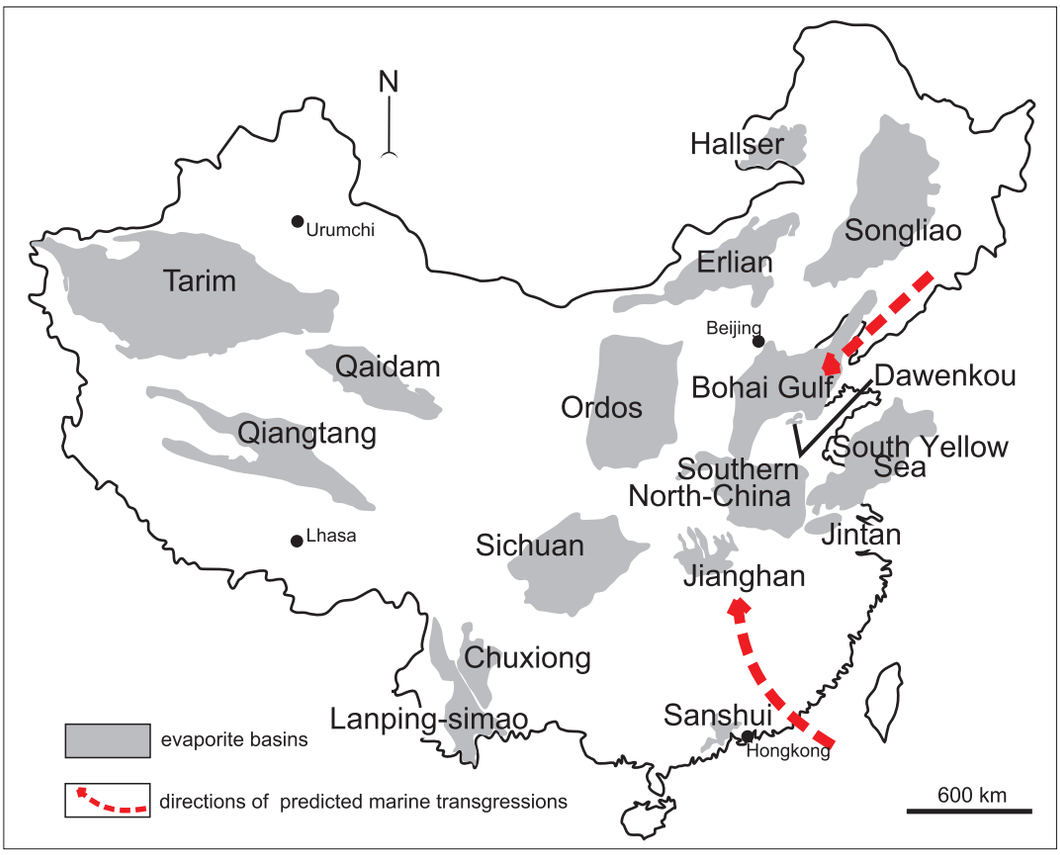

Fig. 1. Location of evaporite basins in China (simplified scheme after Meng et al., 2014)

was taken from a depth of 924.1 m (from the bottom of the second rock salt layer). Anhydrite samples were taken from three anhydrite layers of the salt member to determine the isotopic composition (Fig. 3).

To analyse fluid inclusions, tens of halite plates (1–5 mm thick) were prepared by cleaving crystals along natural planes. Polished sections were examined under a *Polam MPSU-1* binocular microscope, an *Optica 293 B* optical microscope, and a *LEO 1530 VP* scanning electron microscope. The inclusions were classified based on morphology, size, phase composition, and position within the crystal. Additionally, fracture networks and the composition and spatial distribution of solid inclusions were analysed. Primary fluid inclusions were identified using diagnostic criteria, including shape, internal location, phase content, and presence of gas bubbles.

The determination of the ion content in the inclusion brines was carried out using the ultramicrochemical ("glass capillary") method. This method involves the removal of certain ions from the brine into the precipitate with appropriate reagents. Fluids were extracted with glass capillaries (200–250 μm in diameter) with conical tips (4–9 μm), then analysed via selective ion precipitation. In a 30–40 μm fluid inclusion, only one ion can be determined using this method. Therefore, 3–6 inclusions of the same type and size are required to characterize the brine's chemical composition fully. Due to the high concentration of ions in most of the brines studied, 2–4 determinations of the content of individual ions could be conducted in 70–100 μm fluid inclusions. For this, small volumes of brine were collected into several capillaries, followed by dilution (after measurement) in capillaries containing distilled water. The sequence of methodological operations of the ultramicrochemical method has been described in detail (Petrychenko, 1973; Galamay et al., 2020). The minimum concentrations required for the determination of K^+, Mg^{2+} and SO_4^{2-} are 0.8, 1.0, and 0.5 g/L, respectively. The analytical precision varies for each ion: for K^+, it is 1–24%; for Mg^{2+} – 1–6%; and SO_4^{2-} – 2–8% (Galamay et al., 2020).

To determine the pressure inside fluid inclusions, halite was dissolved in a 50% aqueous glycerin solution, which allows for observing the slow process of mineral dissolution. According to Boyle's law, the pressure in the inclusion approximately corresponds to the ratio of the gas volume after opening the inclusion to its initial volume.

The method for analysing sulphur isotopes was modified after Halas and Szaran (1999). Approximately 15 mg of $CaSO_4$ was mixed with 150 mg of $NaPO_3$ and combusted in the presence of 150 mg of copper turnings at 750°C for 15 minutes. The resulting SO_2 was purified in a vacuum line. The analyses were conducted at the Institute of Geology and Geophysics, Chinese Academy of Sciences (IGGCAS), using a *Finnigan Delta S* gas source mass spectrometer. Sulphur isotope results are generally reproducible within ±0.3‰. The $\delta^{18}O$ values were calculated by normalizing the $^{18}O/^{16}O$ ratio in the sample to the Vienna Standard Mean Ocean Water (VSMOW) value. All obtained values were reproducible to within 0.2‰.

RESULTS

Halite samples from the basin exhibit well-developed chevron (bottom-growth) textures. Chevron halite has been identi-

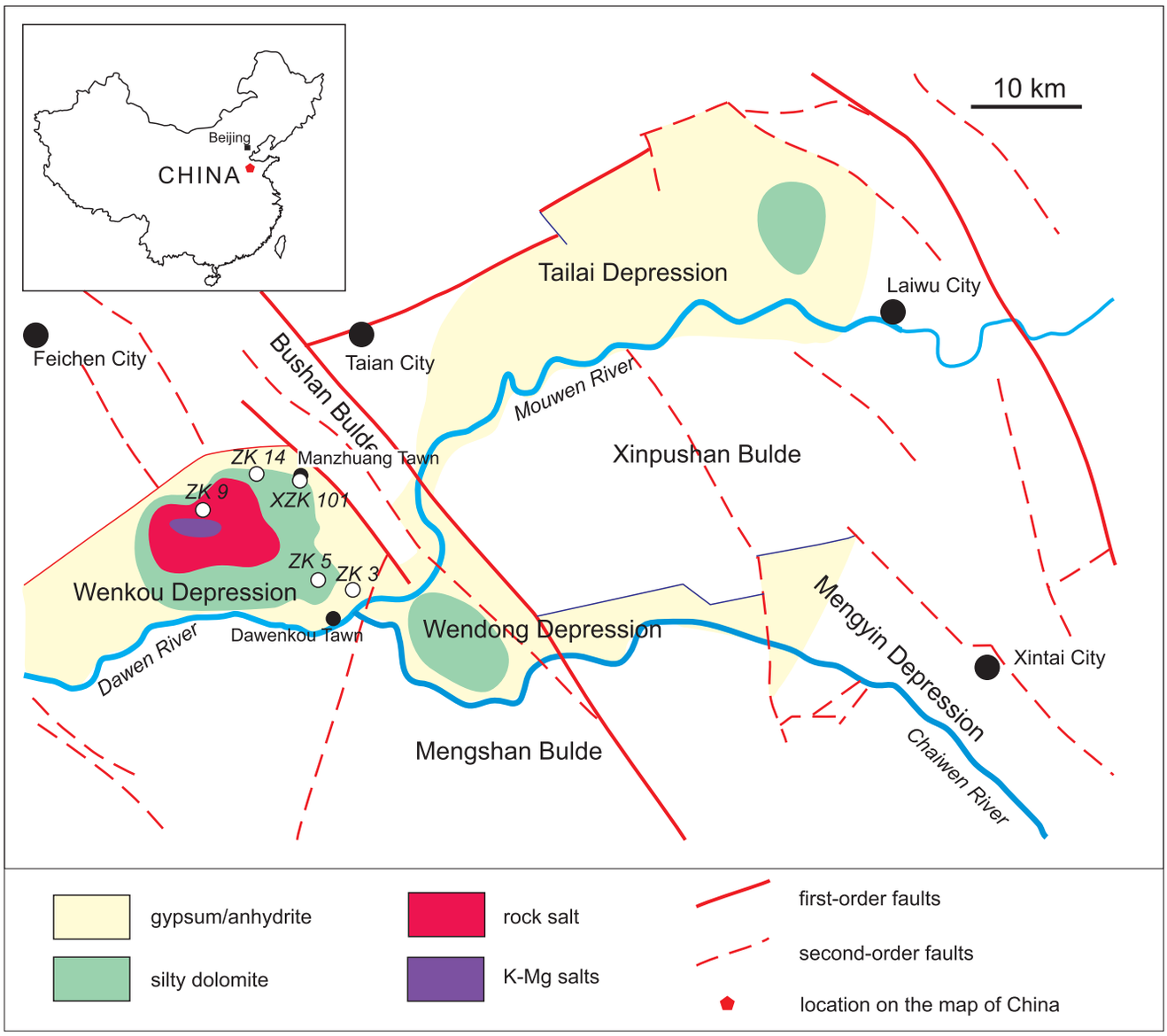

Fig. 2. Schematic facies map of evaporites in the Dawenkou Basin

fied in several samples, showing distinct variations in the distribution and size of fluid inclusions.

In the chevrons of sample DWK-09, large (40–150 μm) fluid inclusions are evenly distributed within inclusion-rich sedimentary zones. In contrast, in sample DWK-07, large fluid inclusions are mainly located at a certain distance from the chevron axis. In some parts of the chevrons, sedimentary zones composed of small (<4 μm) inclusions alternate with zones containing large inclusions (Fig. 4). Single-, two-, and multiphase fluid inclusions have been identified in halite. The multiphase inclusions in brine may contain several components: gas, algae, terrigenous material, small anisotropic crystals, and liquid hydrocarbons. Fluid inclusions filled with liquid hydrocarbons have been identified (Fig. 5). The fluid inclusions in halite are cubic, nearly cubic, or irregular in shape. They occur within the zones of sedimentary textures, randomly distributed in water-clear halite, along the cleavage planes of the mineral, and along a system of numerous cross-cutting fractures (Fig. 6).

Sample DWK-07 is characterized by the presence of a gas phase in most inclusions; however, single-phase inclusions are found along the cleavage planes of the mineral and along fracture planes (Fig. 5). In sample DWK-09, the inclusions do not contain a gas phase, except in some large inclusions. The pressure within the inclusions ranges from close to one atmosphere in sedimentary halite to tens of atmospheres in recrystallized halite.

The range of homogenization temperatures of gas-liquid inclusions in samples DWK-09 and DWK-07 is 33.3–45.2°C and 34.0–63.4°C, respectively (Table 1).

The chemical composition of the brines of primary and secondary inclusions is shown in Table 2.

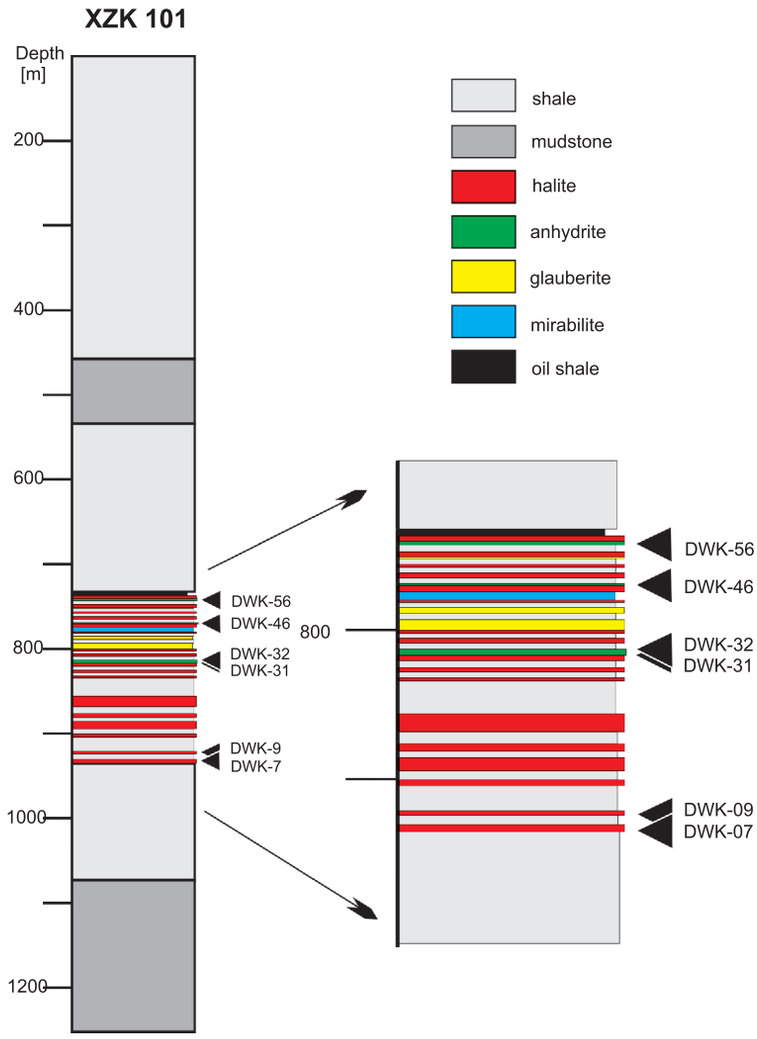

Fig. 3. Lithological column of borehole XZK 101 with sampling locations

Values of $\delta^{34}S$ of the Wenkou Depression anhydrite range from +10.9 to +35.7‰ (CDT), and values of $\delta^{18}O$ of the anhydrite range from +14.7 to +19.4‰ (VSMOW) (Table 3).

INTERPRETATION AND DISCUSSION

HOMOGENIZATION TEMPERATURE OF GAS-LIQUID INCLUSIONS IN SEDIMENTARY HALITE

Single-phase fluid inclusions observed in halite at room temperature indicate crystal growth at temperatures <34–45°C (Kovalevich, 1978; Galamay et al., 2023). Such inclusions are characteristic of both modern salt lakes and many ancient evaporite sequences (Roberts and Spencer, 1995; Galamay et al., 2021a). A gas phase within these inclusions can be induced by cooling halite to –1 to –30°C.

Thermometric studies typically consider only the maximum homogenization temperatures within each growth zone (Acros and Ayora, 1997; Lowenstein et al., 1998). In halite crystallized from brines at temperatures >42–45°C, inclusions are gas-liquid at room temperature (Kovalevich, 1978; Galamay et al., 2023). Experimental data show that homogenization occurs at temperatures lower than crystallization, with ΔT increasing at higher crystallization temperatures (Fig. 8).

Accordingly, the crystallization temperature of DWK-09 halite is estimated at ~45°C, whereas that of WK-07 is ~64°C. The limited presence of a gas phase in inclusions from DWK-09 reflects its relatively low crystallization temperature, a feature also observed in halite from the Tuz Gölü Basin (Galamay et al., 2023).

INFLUENCE OF TECTONIC AND P–T FACTORS ON SALT DEPOSITS

Due to the overprinting of sedimentary chevron textures by numerous multidirectional fractures, it is often impossible to visually distinguish different genetic types of inclusion when they exhibit comparable phase ratios as well as similar shapes and sizes. Some cracks remain open, whereas others are sealed; therefore, the chemical composition of the inclusions represents the only reliable criterion for their differentiation (Fig. 9). These fracture systems formed in response to tectonic activity and acted as pathways for fluid migration (including hydrocarbons) into halite crystals, during which the intersected inclusions underwent modifications of their original chemical composition. A characteristic feature of primary inclusions within each growth zone of sedimentary halite is their uniform ionic composition (Galamay et al., 2020). At later stages, halite recrystallization proceeded under elevated pressures, several tens of times higher than atmospheric pressure.

The combined influence of tectonic and P–T factors on salt deposits is also reflected in the migration traces of large fluid inclusions, as well as in the fragmentation of solid anhydrite inclusions within halite (Fig. 10).

CHEMICAL COMPOSITION OF FLUID INCLUSIONS

The contents of K^+, Mg^{2+}, and SO_4^{2-} in the brines range between 27.6–32.9 g/L, 32.7–41.5 g/L, and 30.7–66.6 g/L, respectively. The chemical composition of post-sedimentary brines (non-primary inclusions in Table 2) is characterized by large differences in the concentrations of the main ions, indicating a repeated process of recrystallization of the deposits. Within the salt stratum, post-depositional brines of the following compositions circulated:

- with a sharply increased (relative to evaporite brine) content of K^+, Mg^{2+}, and SO_4^{2-};
- with an increased content of K^+ and Mg^{2+} alongside reduced SO_4^{2-};
- with a reduced content of K^+ and increased contents of Mg^{2+} and SO_4^{2-};
- with a significantly reduced concentration of K, Mg and SO_4^{2-}-ions.

In the composition of brines of individual inclusions, the Mg^{2+} content is exceptionally high (see Table 2).

The brines of inclusions in which a liquid hydrocarbon phase has been identified differ in ionic ratios from the brines of pri-

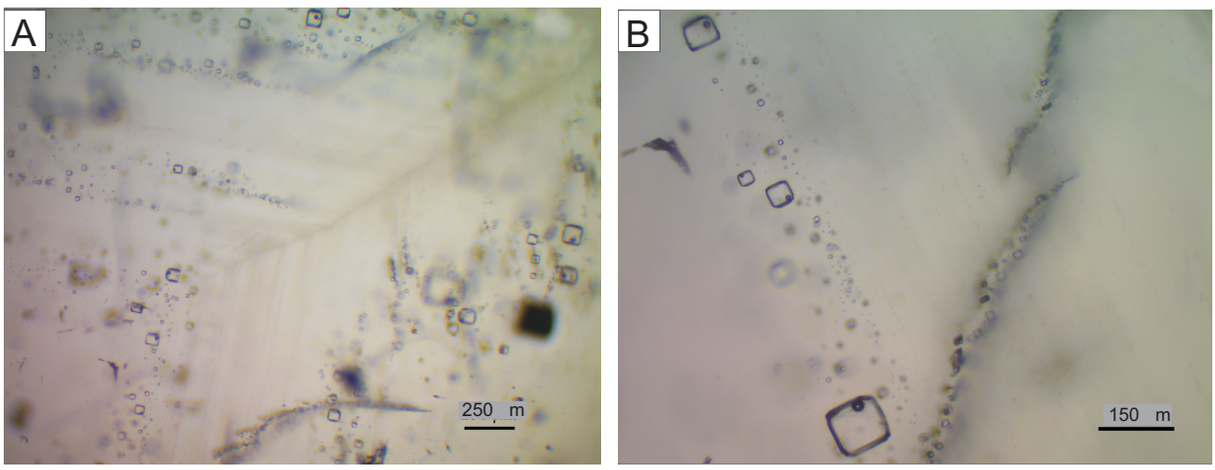

Fig. 4. Chevron textures in sample DWK-07

A – large fluid inclusions are mainly located at a certain distance from the axis of the sedimentary structure;
B – zones composed of small inclusions alternate with zones containing large inclusions

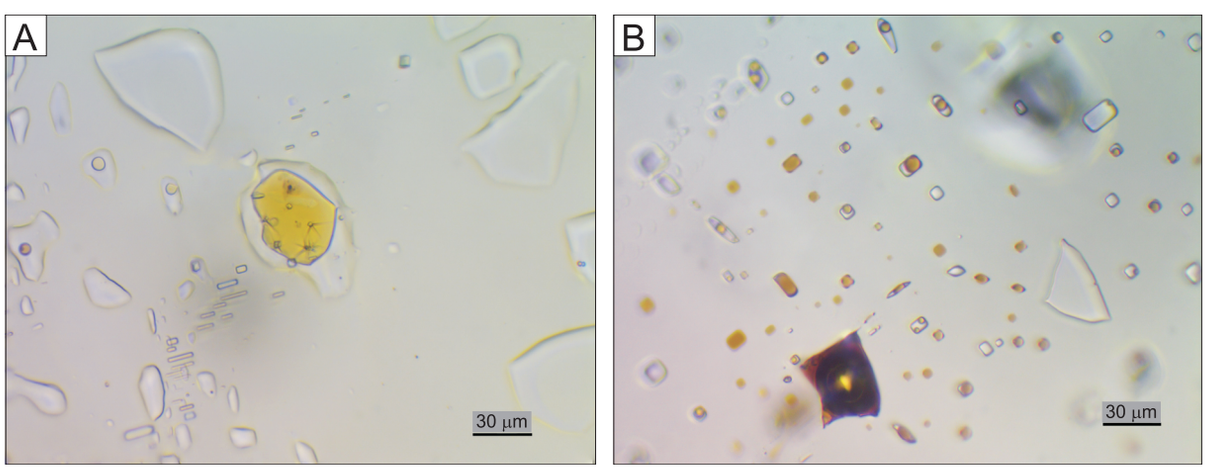

Fig. 5. Liquid hydrocarbons in secondary fluid inclusions in halite, sample DWK-07

A – yellow colorued; **B** – brown-colorued

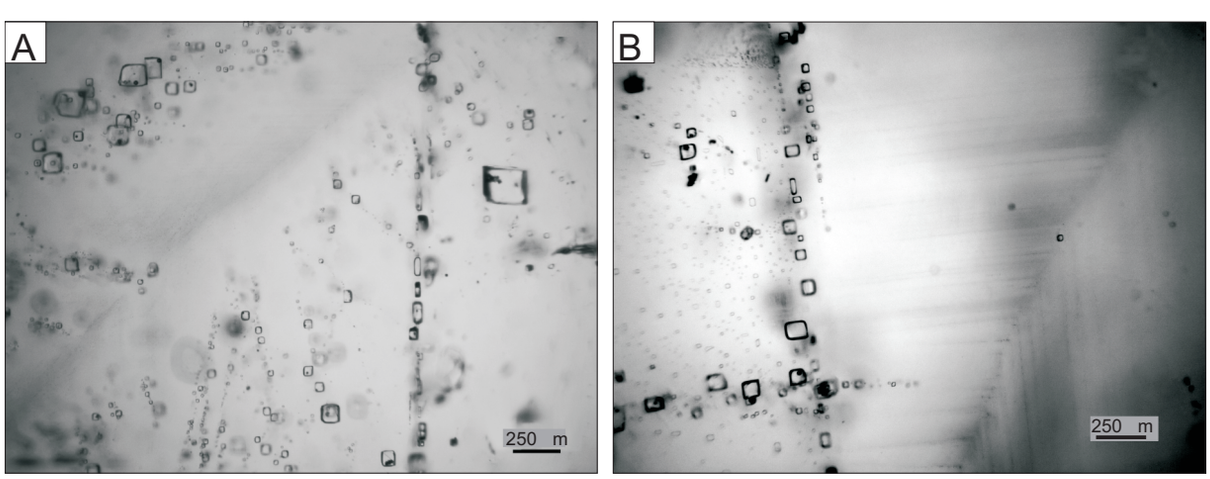

Fig. 6. Cracks in the halite of sample DWK-07

A – multidirectional cracks in the sedimentary texture; **B** – cracks along the perimeter of the crystal and recrystallized halite

Table 1

Homogenization temperatures of gas-liquid inclusions in halite of the Wenkou Depression

Sample	Homogenization temperature (T_{hom}) [°C]	Maximum homogenization temperature (T_{max}), [°C]
DWK-09	33.3, 35.3, 39.3, 40.4, 40.4, 44.1, 44.8, 45.2	45.2
DWK-07	34.0, 38.7, 47.1, 51.2, 56.3, 57.5, 58.9, 63.1, 63.4	63.4

Table 2

Chemical composition of fluid inclusion solutions in halite of the Wenkou Depression of the Dawenkou Basin

No	Inclusion size [μm]	Content, g/L (average value in brackets)			Characteristics of the fluid inclusions
		K^+	Mg^{2+}	SO_4^{2-}	
Sample DWK-09, depth 924.1 m					
1	100	–*	–	120.0, 118.1 (119.1)	single-phase liquid inclusion
2	120	56.2	80.5	124.6	ditto
3	80**	33.6, 27.4, 31.2 (30.5)	40.0	–	ditto
4	125**	25.6	–	58.4, 59.1 (58.8)	two-phase (brine + spherical algal cells; Fig. 7)
5	130**	24.1	42.5	68.3, 79.2 (73.8)	ditto
6	105**	–	38.2	71.0	ditto
7	70**	–	–	61.3, 59.4 (60.4)	single-phase liquid inclusion
8	120**	30.1	45.3	67.3, 70.9 (69.1)	two-phase (brine + small xenogenic crystals)
9	100	–	21.0, 16.0 (18.5)	2.5	two-phase (brine+gas) fluid inclusion
10	70	–	106.0	–	single-phase liquid inclusion
11	80	–	107.8, 104.1 (106.0)	–	ditto
12	175	52.1	55.7, 58.3 (57.0)	31.4, 35.2 (33.3)	fluid inclusion with multiple globules of liquid hydrocarbons
Sample DWK-07, depth 935.3 m					
13	220	–	45.1, 43.6 (44.4)	–	multiphase (brine+gas+small xenogenic crystals) inclusion
14	110**	32.8, 34.6 (33.7)	30.3	25.6, 30.1 (27.9)	two-phase (brine+gas) fluid inclusion
15	125**	32.1	35.1	32.8, 34.2 (33.5)	ditto
16	200	24.1, 26.0 (25.1)	74.8	125.3, 116.2 (120.8)	multiphase (brine+gas+liquid hydrocarbons+small xenogenic crystals) fluid inclusion

* – not measured, ** – primary fluid inclusions

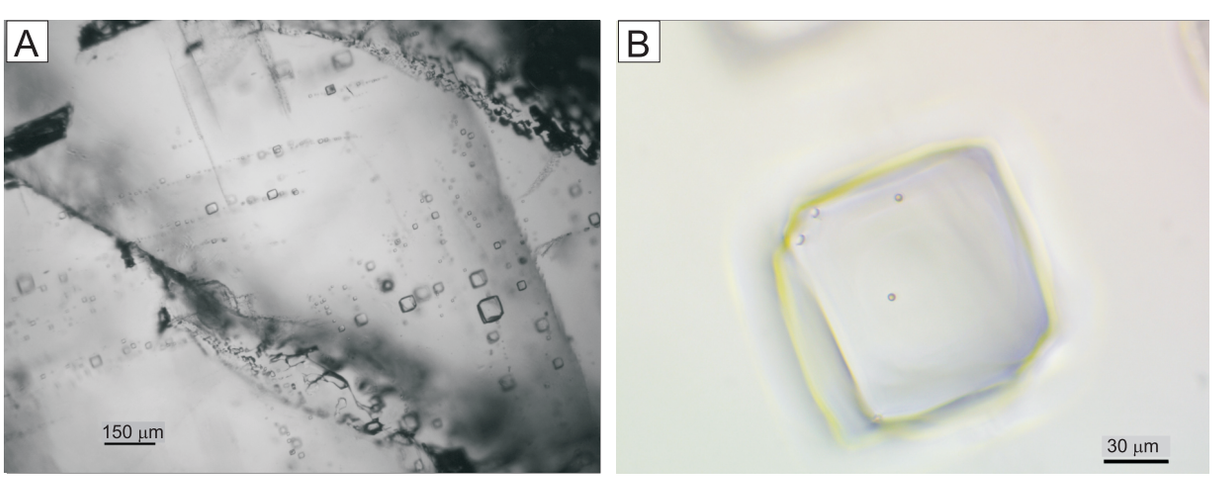

Fig. 7. Primary fluid inclusions in the DWK-09 sample used for chemical analysis of brines

A – general view of the chevron texture; **B** – fragment of the lower right part of the crystal shown in Figure 7A, where large inclusions containing spherical algal cells occur

Table 3

Sulphur isotopic composition of anhydrite from the salt-bearing stratum of the Wenkou Depression

Sample	Lithology	Depth [m]	$\delta^{34}S$ [‰]	$\delta^{18}O$ [‰]
DWK-31	anhydrite	820.0	29.4	19.4
DWK-32	–//–	816.8	28.9	16.5
DWK-46	–//–	770.7	35.7	17.9
DWK-56	–//–	743.06	10.9	14.7

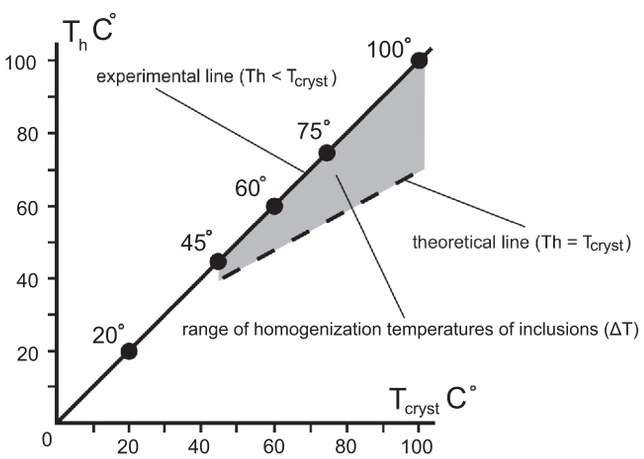

Fig. 8. Graph showing the relationship between the homogenization temperature (Th) of fluid inclusions in synthetic halite crystals and the crystallization temperature (T_{cryst}) (Kovalevich, 1978)

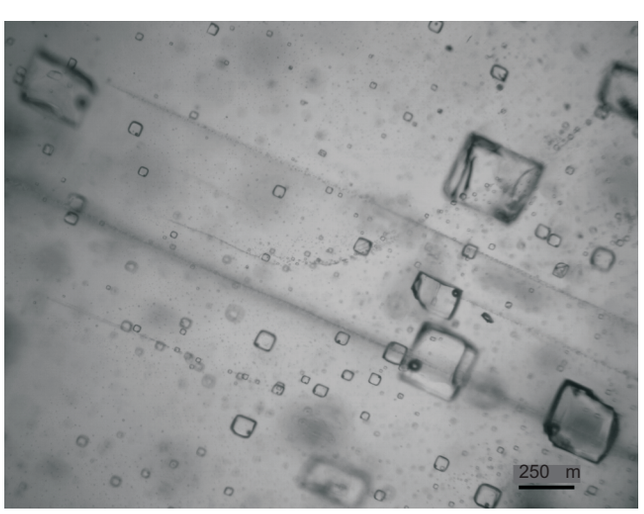

Fig. 9. Fractures in halite (parallel lines) intersect primary (?) fluid inclusions, sample DWK-07

mary inclusions, particularly from those primary inclusions that contain algal cells (see Table 2). This observation is important because similar phenomena in fluid inclusions in halite are interpreted either exclusively as oil or as algal cells (Benison, 2019; Galamay et al., 2021b; Gibson and Benison, 2023). Visual differentiation of hydrocarbon phases from algal cells is difficult because the sizes of hydrocarbon droplets and algal cells are commonly similar, and both lack internal structural organization (Fig. 11).

SALT MINERALOGENESIS

Of the salt minerals, in addition to halite, those found in the Dawenkou Basin include the following: glauberite, thenardite, polyhalite, loewite, vanthoffite, picrimerite, kieserite, aphthitalit and langbeinite.

Considering the mineral composition of the salts of the Dawenkou Basin and the data on the chemical composition of fluid inclusions in the halite, the brines of the basin can be characterized as Na-Mg-K-Cl-SO_4 brines of the sulphate-magnesium subtype of continental or continental-marine halogenation (Stankevich et al., 1991). Sedimentation of potassium-magnesium salts did not take place in the area investigated. For epsomite to precipitate, the Mg^{2+} concentration in brines must exceed 73 g/L, and the SO_4^{2-} content must be over 90 g/L; for sylvite to precipitate, the K^+ content must exceed 33 g/L (Valyashko, 1962; McCaffrey et al., 1987). As a result of the inflow of $Ca(HCO_3)_2$-enriched waters into the basin, the precipitation of either gypsum or glauberite occurred, depending on the Ca/Na ratio of the basin's sedimentary brines. In the lithological column of the area studied, anhydrite and glauberite are found at different depths, indicating fluctuations in the Ca/Na ratio of the sedimentary brines. Evidently, the more than twofold decrease in SO_4^{2-} content in sample DWK-7 (compared to its concentration in sample DWK-9) is primarily related to the precipitation of calcium sulphate, crystals of which are present in the halite studied. The precipitation processes of gypsum and glauberite are characteristic of salt-forming basins (Galamay et al., 2023).

In the lithological column of the area studied, the evaporite minerals identified include halite, anhydrite, mirabilite and glauberite. However, the sedimentary brines in this zone are characterized by elevated concentrations of K^+, Mg^{2+} and SO_4^{2-}, typical of the final stages of halite precipitation. This suggests that, in addition to halite and sodium/calcium sulphates (mirabilite, glauberite, and gypsum), magnesium sulphates (e.g., hexahydrite) and potassium chlorides (e.g., sylvite) may have precipitated in adjacent areas of the basin where sedimentation conditions were favourable for their formation. Gypsum precipitated under bottom conditions of the basin, where brines had reached the stage of sylvite precipitation, was transformed into polyhalite (Petrichenko, 1988).

The distribution of data points representing the chemical composition of certain post-sedimentary brines (with fully determined ionic compositions in individual large inclusions) indicates that their chemistry is both inherited from sedimentary brines and significantly modified by post-sedimentary processes (Fig. 12). Brines with anomalously high magnesium contents (up to 106 g/L), identified in inclusions, are likely residual brines (reaction products) formed during the transformation of unstable sedimentary hexahydrite and sylvite into langbeinite (Khodkova, 1968). These brines migrated into lower-pressure zones and left the potassium-bearing layers of areas adjacent to the site studied via fracture systems. The formation of langbeinite and kieserite in the basin was promoted by elevated temperatures and high pressures during the post-sedimentary stage of deposit evolution.

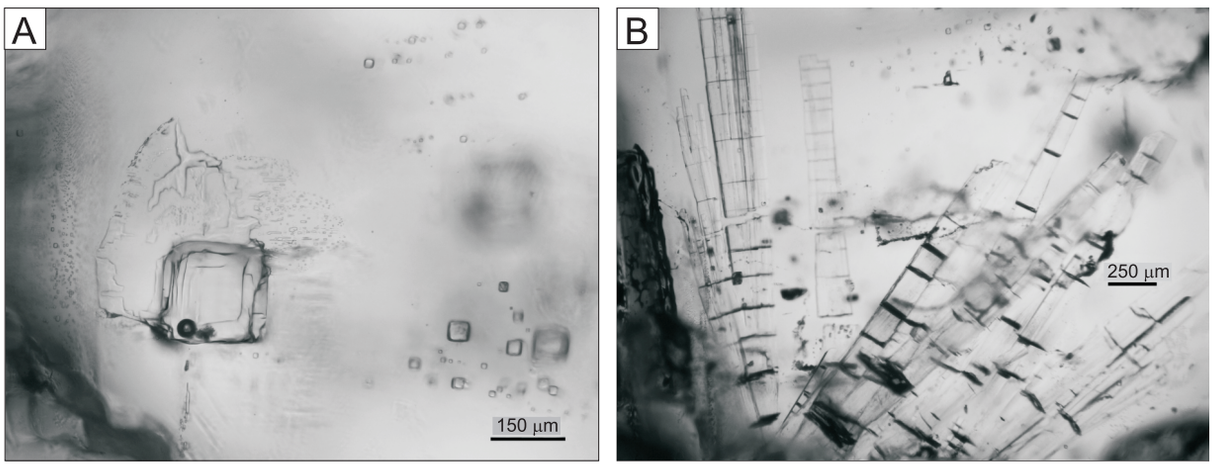

Fig. 10. The effect of post-sedimentation factors on salt-bearing deposits

A – movement of a large inclusion due to the action of a thermal gradient, DWK-09 sample; **B** – elongate anhydrite solid inclusions in halite, showing fracturing caused by brittle deformation, sample DWK-07

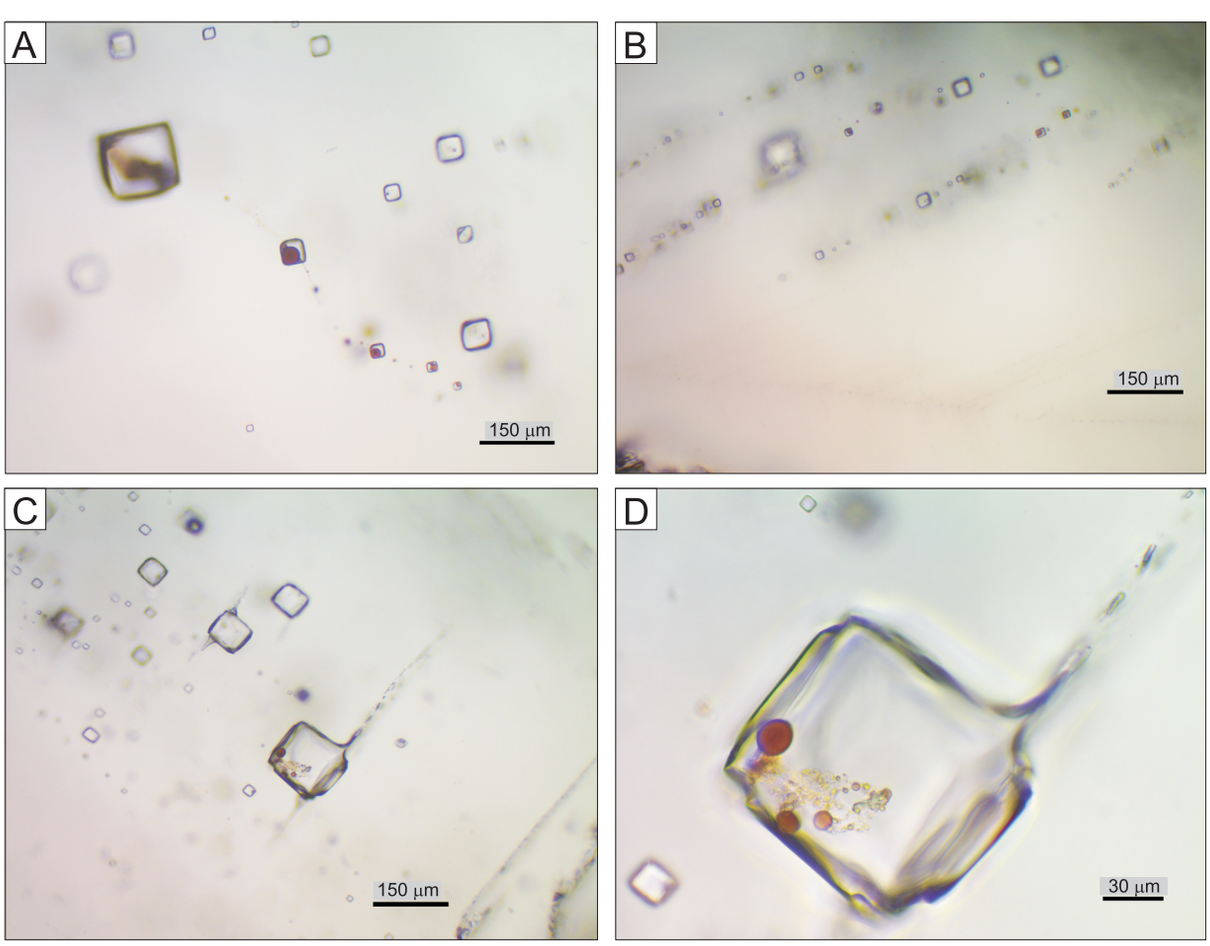

Fig. 11. Small spherical structures in fluid inclusions in halite

A – liquid hydrocarbons ranging from 3 to 35 μm in size, brown in numerous inclusions along a healed fracture, sample DWK-07; **B** – brown spherical structures measuring 3–12 μm in size (liquid hydrocarbons or algal cells?) in the sedimentary halite zone, sample DWK-09; **C, D** – algal cells measuring 2–20 μm in size, brown and light yellow (the larger ones are elliptical and more intensely coloured) in a large refilled inclusion within the sedimentary halite texture, sample DWK-09

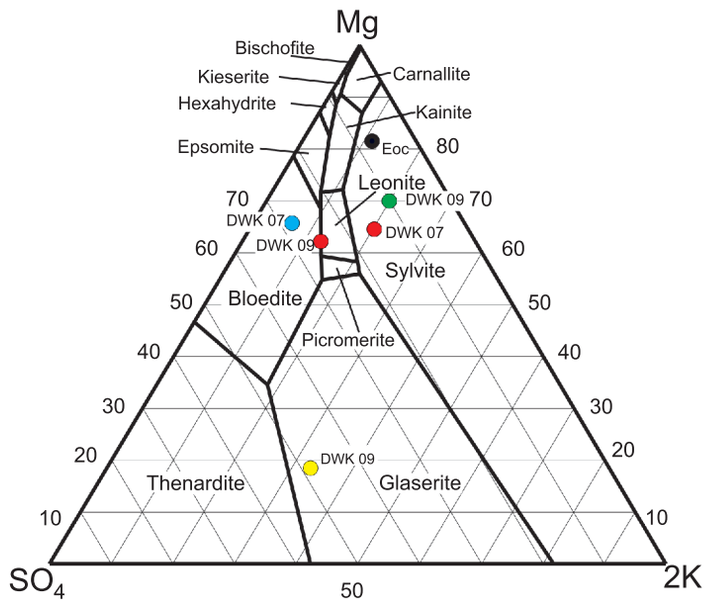

Fig. 12. Brine compositions of fluid inclusions in sedimentary halite of the Dawenkou Basin on a Jänecke diagram (reference) of the Na-K-Mg-SO_4-Cl-H_2O system (Eugster et al., 1980, relative to Eocene evaporite brine (Eoc) under conditions just before halite deposition (Ayora et al., 1994)

Considering the presence of halite in the lithological column of the XZK 101 well and according to the data obtained on the chemical composition of the brines of the inclusions in the halite, the boundaries of both the halite and potash facies on the existing facies maps (see Fig. 2) should be revised.

SOURCES OF SALTS

Micropalaeontological and sedimentological data from previous studies (Li, 1986; Ren et al., 2000; Wu and Ren, 2004; Zhu et al., 2015), along with our data on the chemical composition of sedimentary brines, do not exclude the influence of marine transgressions on salt formation in the Dawenkou Basin. In typical Eocene marine brines with a K^+ content of 16.4 g/L, the Mg^{2+} content is 36.3 g/L, and SO_4^{2-} is 12.5 g/L (Ayora et al., 1994). The brines. studied differ from marine ones in having a slightly lower Mg^{2+} content and a significantly higher SO_4^{2-} content. Therefore, the brine composition points are below Eocene seawater's composition point on the K-Mg-SO_4 ternary diagram (Fig. 12).

The analysis of $\delta^{34}S$ and $\delta^{18}O$ of anhydrite from Phanerozoic marine strata, alongside the isotopic composition of dissolved sulphate from modern river waters of the study area, reveals the following:

1. In Cambrian anhydrite, $\delta^{34}S$ is highest, reaching +35.5‰, while in the Permian it decreases to 8.4‰ (Claypool et al., 1980; Galamay et al., 2016). In Eocene marine evaporites, the value of this indicator ranges from +10.9 to +22.4‰ (Yao et al., 2019). In Paleocene sulphates of marine origin of the Tarim Basin, western China, $\delta^{34}S$ is +16.5–+17.9‰ (Xu et al., 2020).

2. The minimum values of $\delta^{18}O$ (+10‰) are recorded in Permian anhydrite, while the maximum values (+17‰) are found in Devonian and Carboniferous strata. In Cambrian and Paleogene/Neogene anhydrite, this indicator ranged from +10.7 to +15.7‰ and from +10.8 to +14.1‰, respectively (Claypool et al., 1980).

3. The isotopic composition of dissolved sulphate in the modern Yellow River in North China is as follows: $\delta^{34}S(SO_4)$ ranges from +7.9 to +12.5‰, and $\delta^{18}O(SO_4)$ ranges from +4.8 to +8.4‰ (Zhang et al., 2013).

The $\delta^{34}S$ and $\delta^{18}O$ values of Eocene marine anhydrite (+10.9 to +22.4‰ and +10.8 to +14.1‰, respectively) only partially fall within the range of these parameters for anhydrite in the basin studied (+10.9 to +35.7‰ and +14.7 to +19.4‰, respectively). The characteristic values of the anhydrite isotope composition parameters described above are shown in Figure 13.

Based on the results of the isotopic and thermobarogeochemical study, the main source of sulphate in the basin was Cambrian (gypsum and halite) and Ordovician (gypsum) salt-bearing deposits, which were eroded by surface waters. These ancient evaporites are abundant in the surrounding area of the Yi-Meng Mountains (Liu et al., 2003; Xiao et al., 2010).

This leaching process did not cause sulphur isotope fractionation; however, the $\delta^{34}S$ value of the solvent water was significantly influenced by the $\delta^{34}S$ of the rocks and minerals being leached. Thus, the increase in the $\delta^{34}S$ of basin anhydrite of up to +35.7‰ resulted from the redeposition of Cambrian sulphate rocks. When mixed with lighter marine or river water sulphate, the leached sulphate exhibited an isotopically heavier sulphur composition that was intermediate compared to that of seawater or river water.

The isotopic analysis described, of sulphates and the chemical composition data of sedimentary brine, do not exclude the

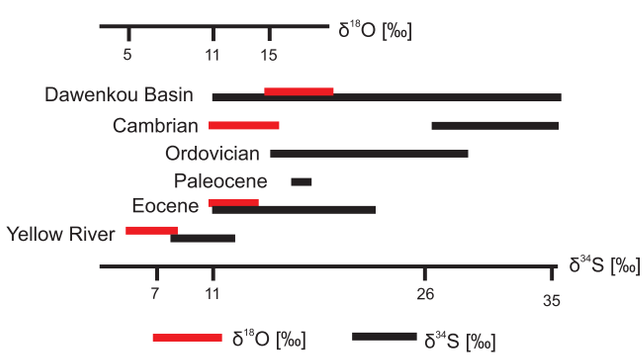

Fig. 13. The sulphur and oxygen isotopic composition of anhydrite from the Dawenkou Basin by comparison with the corresponding values for the Cambrian (Claypool et al., 1980), Ordovician (Claypool et al., 1980), Paleocene (Xu et al., 2020), Eocene (Yao et al., 2019), and Yellow River water (Zhang et al., 2013)

possibility of marine transgressions influencing halogenesis in the basin. Positioning the chemical composition points of primary fluid inclusions in halite, located below the Eos point in Figure 12, is primarily due to the influx of a significant amount of sulphate ions into the basin from the leaching of gypsum on land.

CONCLUSIONS

Study of primary and secondary inclusions in halite from the Dawenkou Basin made it possible to determine the genesis of the basin brines and specific features of mineral formation:

1. The chemical composition of sedimentary brines reveals concentrations of potassium, magnesium, and sulphate ranging from 27.6 to 32.9 g/L, 32.7 to 41.5 g/L, and 30.7 to 66.6 g/L, respectively.

2. The chemical composition of the post-sedimentary brine exhibits wide variations in the concentrations of major ions, indicating repeated recrystallization processes of the deposits. Within the salt-bearing strata, the following types of brine compositions were identified:

- with significantly elevated concentrations of K^+, Mg^{2+} and SO_4^{2-} compared to sedimentary brines;
- with increased concentrations of K^+ and Mg^{2+} and decreased SO_4^{2-};
- with decreased K^+ and elevated Mg^{2+} and SO_4^{2-} concentrations;
- with significantly reduced concentrations of all major ions.

3. Potassium-magnesium salts did not crystallize in the area of the basin studied. Although the brine reached the stage of sylvite precipitation, the inflow of calcium-rich continental waters promoted gypsum dissolution, followed by the transformation of gypsum into polyhalite under bottom conditions.

4. Recrystallization of halite occurred under elevated pressure, which exceeded atmospheric pressure by several tens of times. Brines with anomalously high magnesium contents are interpreted as residual brines (reaction products) resulting from the formation of langbeinite through the transformation of unstable sedimentary hexahydrite and sylvite. These brines likely migrated from the potash-bearing layers of adjacent parts of the basin toward the studied area (a zone of lower pressure) through fracture systems.

5. The data obtained on the chemical composition of sedimentary brines and the $\delta^{34}S$ and $\delta^{18}O$ values of anhydrite do not rule out the influence of marine transgressions on halogenesis in the basin studied. However, the main source of sulphate in its brines was the gypsum of the surrounding land.

Acknowledgements. The authors sincerely thank C. Eastoe for his help in improving the English language and for the valuable comments that enhanced the quality of the article. This research was supported by the National Key Research and Development Program of China (no. 2023YFE0104000). The article was also prepared for the AGH University project number 16.16.140.315 (KB).

REFERENCES

Acros, D., Ayora, C., 1997. The use of fluid inclusions in halite as environmental thermometer: an experimental study. Proceedings of the XIVth European Current Research on Fluid Inclusions (XIV ECROFI) (eds. M.C. Boiron and J. Pironon): 10–11. Université de Lorraine – CNRS: Nancy, France, 1–4 July 1997.

Ayora, C., Garcia-Veigas, J., Pueyo, J.J., 1994. The chemical and hydrological evolution of an ancient potash-forming evaporite basin as constrained by mineral sequence, fluid inclusion composition, and numerical simulation. Geochimica et Cosmochimica Acta, **58**: 3379–3394; https://doi.org/10.1016/0016-7037(94)90093-0

Bąbel, M., Schreiber, B.C., 2014. Geochemistry of evaporites and evolution of seawater. Treatise on Geochemistry, **9**: 483–560; https://doi.org/10.1016/B978-0-08-095975-7.00718-X

Benison, K.C., 2019. How to search for life in Martian chemical sediments and their fluid and solid inclusions using petrographic and spectroscopic methods. Frontiers in Environmental Science, **7**, 108; https://doi.org/10.3389/fenvs.2019.00108

Benison, K.C., Goldstein, R.H., 1999. Permian paleoclimate data from fluid inclusions in halite. Chemical Geology, **154**: 113–132; https://doi.org/10.1016/S0009-2541(98)00127-2

Claypool, G.E., Holser, W.T., Kaplan, I.R., Sakai, H., Zak, I., 1980. The age curves of sulfur and oxygen isotopes in marine sulfate and their mutual interpretation. Chemical Geology, **28**: 199–260; https://doi.org/10.1016/0009-2541(80)90047-9

Drever, J.I., 1997. The Geochemistry of Natural Water: Surface and Groundwater Environments. 3rd Edition. Prentice Hall, New Jersey.

Eugster, H.P., Harvie, C.E., Weare, J.H., 1980. Mineral equilibria in a six-component seawater system, Na-K-Mg-Ca-SO_4-Cl-H_2O, at 25°C. Geochimica et Cosmochimica Acta, **44**: 1335–1347; https://doi.org/10.1016/0016-7037(80)90093-9

Galamay, A.R., Meng, F., Bukowski, K., Ni, P., Shanina, S.N., Ignatovich, O.O., 2016. The sulphur and oxygen isotopic composition of anhydrite from the Upper Pechora Basin (Russia): new data in the context of the evolution of the sulphur isotopic record of Permian evaporites. Geological Quarterly, **60**: 990–999; https://doi.org/10.7306/gq.1309

Galamay, A.R., Bukowski, K., Sydor, D. V., Meng, F., 2020. The Ultramicrochemical Analyses (UMCA) of Fluid Inclusions in Halite and Experimental Research to Improve the Accuracy of Measurement. Minerals, **10**, 823; https://doi.org/10.3390/min10090823

Galamay, A.R., Poberezhsky, A.V., Hryniv, S.P., Sydor, D., Iaremchuk, J., Maksymuk, S., Oliyovych-Hladka, O., Bilyk, L., 2021a. Geochemical features of Eurasian evaporite formations in the context of the evolution of the chemical composition of seawater during the Phanerozoic. Geology and Geochemistry of Combustible Minerals, (183–184): 110–129; https://doi.org/10.15407/ggcm2021.01-02.110

Galamay, A.R., Maksymuk, S.V., Sydor, D.V., 2021b. Geochemical features of the influence of oil and gas deposits on the covering salts of the Carpathian oil and gas province (in Ukrainian with English summary). In: VII International Scientific and Practical Conference "Subsoil Use in Ukraine. Investment Prospects", **2**: 100–105. Lviv, Ukraine.

Galamay, A.R., Karakaya, M.Ç., Bukowski, K., Karakaya, N., Yaremchuk, Y., 2023. Geochemistry of brine and paleoclimate reconstruction during sedimentation of Messinian salt in the Tuz Gölü Basin (Türkiye): insights from the study of fluid inclusions. Minerals, **13**, 171; https://doi.org/10.3390/min13020171

Gibson, M.E., Benison, K.C., 2023. It's a trap!: modern and ancient halite as Lagerstätten. Journal of Sedimentary Research, **93**: 642–655; https://doi.org/10.2110/jsr.2022.110

Halas, S., Szaran, J., 1999. Low-temperature thermal decomposition of sulfate to SO_2 for on-line $^{34}S/^{32}S$ Analysis. Analytical Chemistry, **71**: 3254–3257; https://doi.org/10.1021/ac9900174

Hardie, L.A., 1984. Evaporites, marine or non-marine? American Journal of Science, **284:** 193–240; https://doi.org/10.2475/ajs.284.3.193

Horita, J., Zimmermann, H., Holland, H.D., 2002. Chemical Evolution of Seawater during the Phanerozoic: Implications from the Record of Marine Evaporites. Geochimica et Cosmochimica Acta, **66**: 3733–3756; https://doi.org/10.1016/S0016-7037(01)00884-5

Khod'kova, S.V., 1968. Langbeinite of the Pre-Carpathian region and its parageneses (in Russian). Lithology and Mineral Resources, **6**: 73–85.

Kovalevich, V.M., 1978. Physical and Chemical Conditions of Salts Formation in the Stebnyk Potash Deposit (in Russian). Naukova Dumka, Kyiv.

Kovalevich, V.M., 1990. Halogenesis and Chemical Evolution of the Ocean in the Phanerozoic (in Russian). Naukova Dumka, Kyiv.

Kovalevych, V.M., Paul, J., Peryt, T.M., 2009. Fluid inclusions in halite from the Röt (Lower Triassic) salt deposit in Central Germany: Evidence for seawater chemistry and conditions of salt deposition and recrystallization. Carbonates and Evaporites, **24**: 45–57; https://doi.org/10.1007/BF03228056

Kovalevych, V.M., Dudok, I.V., Poberezhsky, A.V., Vovniuk, S., Halamai, A., Hryniv, S., Lytvyniuk, S., Sydor, D., Yaremchuk, Y., 2012. Chemical paleoceanographic indicators for hydrocarbon deposit prediction. Geology and Geochemistry of Combustible Minerals, (3–4): 66–81.

Li, M.H., 1986. Paleoecological analysis of the Early Tertiary oil-bearing sedimentary formation in the Dongpu Depression, North China Diwa Region (in Chinese with English summary). Geotectonics and Metallogeny, **10**: 159–168.

Liu, M.W., Song, W.Q., Xu, J.Q., Zhang, Y.J., Xu, L.J., 2003. Geological characteristics of Cambrian gypsum deposit in Longquan of Yiyuan County (in Chinese with English summary). Geological Journal of Shandong, **19**: 39–42.

Lowenstein, T.K., Hardie, L.A., 1985. Criteria for the recognition of salt-pan evaporites. Sedimentology, **32**: 627–644; https://doi.org/10.1111/j.1365-3091.1985.tb00478.x

Lowenstein, T.K., Li, J., Brown, C.B., 1998. Paleotemperatures from fluid inclusions in halite: method verification and a 100,000 year paleotemperature record, Death Valley, CA. Chemical Geology, **150**: 223–245; https://doi.org/10.1016/S0009-2541(98)00061-8.

Lowenstein, T.K., Timofeeff, M.N., Brenman, S.T., Hardie, L.A., Demiccio, R.V., 2001. Oscillations in Phanerozoic seawater chemistry: evidence from fluid inclusions. Science, **294**: 1086–1088; https://doi.org/10.1126/science.1064280

Lowenstein, T.K., Hardie, L.A., Timofeeff, M.N., Demicco, R.V., 2003. Secular variation in seawater chemistry and the origin of calcium chloride basinal brines. Geology, **31**: 857–860; https://doi.org/10.1130/G19728R.1

McCaffrey, M.A., Lazar, B., Holland, H.D., 1987. The evaporation path of seawater and the coprecipitation of Br and K with halite. Journal of Sedimentary Petrology, **57**: 928–937; https://doi.org/10.1306/212F8CAB-2B24-11D7-8648000102C1865D

Meng, F., Galamay, A.R., Ni, P., Yang, C.-H., Li, Y.P., Zhuo, Q.G., 2014. The major composition of a Middle-Late Eocene Salt Lake in the Yunying Depression of Jianghan Basin of Middle China based on analyses of fluid inclusions in halite. Journal of Asian Earth Sciences, **85**: 97–105; https://doi.org/10.1016/j.jseaes.2014.01.024

Meng, F., Galamay, A.R., Ni, P., Ahsan, N., Rehman, S.U., 2020. Composition of Middle-Late Eocene salt lakes in the Jintan Basin of Eastern China: evidence of marine transgressions. Marine and Petroleum Geology, **122**, 104644; https://doi.org/10.1016/j.marpetgeo.2020.104644.

Petrichenko, O.Y., 1988. Physicochemical Conditions of Sedimentation in Ancient Salt Basins (in Russian). Naukova Dumka, Kyiv.

Petrychenko, O.Y., 1973. Methods of Studying Inclusions in Halogen Rocks Minerals (in Ukrainian). Naukova Dumka, Kyiv.

Petrychenko, O.Y., Kovalevich, V.M., Poberezhskyi, A.V., Vovniuk, S.V., Galamay, A.R., Dudok, I.V., Hryniv, S.P., Khmelevska, O.V., Sydor, D.V., Yaremchuk, Y.V., Oliiovych, O.V., Lytvyniuk, S., 2006. Age-related changes in the chemical composition of oceanic water and their influence on the formation of halogen and bituminous deposits. Geology and Geochemistry of Combustible Minerals, (3–4): 97–118.

Ren, L.Y., Lin, G.F., Zhao, Z.Q., Wang, X.W., 2000. Early Tertiary marine transgression in Dongpu Depression (in Chinese with English summary). Acta Palaeontologica Sinica, **39**: 553–557.

Roberts, S.M., Spencer, R.J., 1995. Paleotemperatures preserved in fluid inclusions in halite, Geochimica et Cosmochimica Acta, **59**: 3929–3942; https://doi.org/10.1016/0016-7037(95)00253-V

Song, S.W., 2010. Rock salt mining and security study of Tai'an Dawenkou Basin (in Chinese with English summary). Geological Chemistry and Mineralogy, **32**: 177–185.

Sonnenfeld, P., Hardie, L.A., 1985. Evaporites, marine or non-marine; discussion and reply. American Journal of Science, **285**: 661–672; https://doi.org/10.2475/ajs.285.7.661

Stankevich, E.F., Batalin, Y.V., Chaikin, V.G., 1991. On the differences between marine and continental halogenic deposits (in Russian). In: Problems of Marine and Continental Halogenesis: 23–30. Nauka, Novosibirsk.

Strakhov, N.M., 1962. Fundamentals of lithogenesis theory (in Russian). Academy of Sciences of the USSR, Moscow.

Valyashko, M.G., 1962. Patterns of deposit salts formation (in Russian). Moscow State University Publishing House, Moscow.

Vovnyuk, S.V., Galamay, A.R., Hryniv, S.P., Dudok, I., Maksymuk, S., Poberezhskyi, A., Sydor, D., Yaremchuk, Y., 2017. Geochemical criteria linking Phanerozoic evaporite and sedimentary formations with hydrocarbon deposits. Geology and Geochemistry of Combustible Minerals, (3–4): 56–75.

Wang, Z.J., Li, Q., Li, Z.C., 2003. Potentiality evaluation of gypsum resource in Dawenkou Basin in Tai'an City and suggestion on ore need prediction and exploration (in Chinese with English summary). Land Resources of Shandong Province, **19**: 23–25.

Wang, H., Han, W.-C., Zhang, G.-Q., Zhang, Y.-M., Wang, M.-Z., Li, S., Cao, M.-Z., Zhang, H.-C., 2022. Paleogene ostracodes from the Dawenkou Basin, East China and their biostratigraphic significance for the age of mineral resources. Palaeoworld, **31**: 131–139; https://doi.org/10.1016/j.palwor.2021.01.007

Wu, T., Ren, L.Y., 2004. The Tertiary seaway and new reservoir probe in Dongpu Depression as well as its surrounded basins (in Chinese with English summary). Acta Palaeontologia Sinica, **43**: 147–154.

Xiao, B.J., Liu, A.T., Zhang, Y.Y., Dong, W.H., 2010. Geological characteristics of Xiaotun gypsum deposits in Zhangfanxiang of Zaozhuang City in Shandong Province (in Chinese with English summary). Land Resources of Shandong Province, **26**: 12–15.

Xu, Y., Cao, Y., Liu, C., Zhang, H., Nie, X., 2020. The history of transgressions during the Late Paleocene–Early Eocene in the Kuqa Depression, Tarim Basin: constraints from C-O-S-Sr isotopic geochemistry. Minerals, **10**, 834; https://doi.org/10.3390/min10090834

Yao, W., Wortmann, U.G., Paytan, A., 2019. Sulfur isotopes – use for stratigraphy during times of rapid perturbations. In: Stratigraphy and Timescales, 4 (ed. M. Montenari): 1–33. Elsevier. https://doi.org/10.1016/bs.sats.2019.08.003

Zhang, D., Huang, X.Y., Li, C.J., 2013. Sources of riverine sulfate in Yellow River and its tributaries determined by sulfur and oxygen isotopes (in Chinese with English summary). Advances in Water Science, **24**: 418–426.

Zhu, M., 2015. Study on the Origin of Salt Deposit in Dawenkou Basin in Shandong Province (in Chinese with English summary). Land Resources of Shandong Province, **31**: 27–30.

Zimmermann, H., 2000. Tertiary seawater chemistry – implications from primary fluid inclusions in marine halite. American Journal of Science, **300**: 3–45; https://doi.org/10.2475/ajs.300.10.723